Tumor and Stem Cell Biology

Cancer Research

Characterization of a Novel PERK Kinase Inhibitor with Antitumor and Antiangiogenic Activity

Charity Atkins[1], Qi Liu[1], Elisabeth Minthorn[1], Shu-Yun Zhang[1], David J. Figueroa[1], Katherine Moss[1], Thomas B. Stanley[3], Brent Sanders[1], Aaron Goetz[2], Nathan Gaul[2], Anthony E. Choudhry[2], Hasan Alsaid[4], Beat M. Jucker[4], Jeffrey M. Axten[1], and Rakesh Kumar[1]

Abstract

The unfolded protein response (UPR) is a signal transduction pathway that coordinates cellular adaptation to microenvironmental stresses that include hypoxia, nutrient deprivation, and change in redox status. These stress stimuli are common in many tumors and thus targeting components of the UPR signaling is an attractive therapeutic approach. We have identified a first-in-class, small molecule inhibitor of the eukaryotic initiation factor 2-alpha kinase 3 (EIF2AK3) or PERK, one of the three mediators of UPR signaling. GSK2656157 is an ATP-competitive inhibitor of PERK enzyme activity with an IC_{50} of 0.9 nmol/L. It is highly selective for PERK with IC_{50} values >100 nmol/L against a panel of 300 kinases. GSK2656157 inhibits PERK activity in cells with an IC_{50} in the range of 10–30 nmol/L as shown by inhibition of stress-induced PERK autophosphorylation, eIF2α substrate phosphorylation, together with corresponding decreases in ATF4 and CAAT/enhancer binding protein homologous protein (CHOP) in multiple cell lines. Oral administration of GSK2656157 to mice shows a dose- and time-dependent pharmacodynamic response in pancreas as measured by PERK autophosphorylation. Twice daily dosing of GSK2656157 results in dose-dependent inhibition of multiple human tumor xenografts growth in mice. Altered amino acid metabolism, decreased blood vessel density, and vascular perfusion are potential mechanisms for the observed antitumor effect. However, despite its antitumor activity, given the on-target pharmacologic effects of PERK inhibition on pancreatic function, development of any PERK inhibitor in human subjects would need to be cautiously pursued in cancer patients. *Cancer Res; 73(6); 1993–2002. ©2012 AACR.*

Introduction

To cope with the relatively extreme conditions of the tumor microenvironment, cancer cells depend on adaptive responses to cope with stress and to continue to proliferate. Multiples lines of evidence have implicated the unfolded protein response (UPR), an endoplasmic reticulum stress sensing/repair pathway, in cell survival and tumor progression (1–3). Stress stimuli that activate UPR include hypoxia, nutrient deprivation, increased protein synthesis, disruption of protein glycosylation (glucose deprivation), decreased luminal endoplasmic reticulum calcium, or changes in endoplasmic reticulum redox status (2, 3). These perturbations result in the accumulation of unfolded or misfolded proteins in the endoplasmic reticulum, triggering a coordinated cellular response to alleviate the impact of the stress and enhance cell survival. Responses include an increase in the level of chaperone proteins to enhance protein refolding, degradation of the misfolded proteins, and translational arrest to decrease the burden of proteins entering the endoplasmic reticulumf. These pathways also regulate cell survival by modulating apoptosis (2–4) and can trigger cell death under conditions of prolonged endoplasmic reticulum stress.

Three endoplasmic reticulum membrane proteins have been identified as primary effectors of the UPR: protein kinase R (PKR)-like endoplasmic reticulum kinase [PERK, also known as eukaryotic initiation factor 2-alpha kinase 3 (EIF2AK3), or pancreatic endoplasmic reticulum kinase (PEK)], inositol-requiring gene 1 α/β (IRE1), and activating transcription factor 6 (ATF6; ref. 2). These proteins are held in the inactive state by binding to the endoplasmic reticulum chaperone, GRP78 (BiP). Accumulation of unfolded proteins in the endoplasmic reticulum leads to release of GRP78 from the luminal stress-sensing domains of the UPR effectors resulting in their activation (5).

PERK is a type I endoplasmic reticulum transmembrane protein containing a stress-sensing domain facing the endoplasmic reticulum lumen and a cytosolic kinase domain (6, 7). Release of GRP78 from the stress-sensing domain of PERK

Authors' Affiliations: [1]GlaxoSmithKline, Oncology R&D; [2]Platform Technology & Science, Collegeville, Pennsylvania; [3]Platform Technology & Science, Research Triangle Park, North Carolina; and [4]Preclinical and Translational Imaging, LAS, King of Prussia, Pennsylvania

Note: Supplementary data for this article are available at Cancer Research Online (http://cancerres.aacrjournals.org/).

Corresponding Author: Rakesh Kumar, GlaxoSmithKline, Oncology R&D, 1250 South Collegeville Road, Collegeville, PA 19426. Phone: 610-917-4855; Fax: 610-917-4181; E-mail: rakesh.2.kumar@gsk.com

doi: 10.1158/0008-5472.CAN-12-3109

results in oligomerization and autophosphorylation (8, 9). PERK phosphorylates the eukaryotic initiation factor 2α (eIF2α) at serine-51 (10). This site is also phosphorylated by other PERK family members [general control nonderepressed 2 (GCN2), protein kinase RNA-activated (PKR), and heme-regulated kinase (HRI)] in response to different stimuli. Phosphorylation of eIF2α converts it to an inhibitor of eIF2B, which hinders the assembly of the 40S ribosome translation initiation complex and consequently reduces the rate of translation initiation. However, translation of certain messages encoding downstream effectors of eIF2α, ATF4, and CAAT/enhancer binding protein (C/EBP) homologous protein (CHOP), which modulate cellular survival pathways, is actually increased upon endoplasmic reticulum stress. A second proposed PERK substrate, Nrf2 (NF-E2-related factor 2), regulates cellular redox potential and contributes to cell adaptation (11). It is thought that the normal function of PERK is to protect secretory cells from endoplasmic reticulum stress. *PERK* knockout mice exhibit diabetes due to pancreatic islet cell death, skeletal abnormalities, and growth retardation (12–14). These features are similar to those seen in patients with Wolcott–Rallison syndrome, who carry inactivating germ line mutations in the *PERK* gene (15, 16).

PERK has also been shown to have endoplasmic reticulum stress independent effects. PERK regulates proliferation of beta cells during embryonic and neonatal development and is essential for viability of acinar cells in mouse exocrine pancreas, neither of which is associated with endoplasmic reticulum stress response (13, 14, 17). PERK is also required for endoplasmic reticulum functions including proinsulin trafficking and quality control in beta cells (18, 19). Similarly, PERK modulates proliferation and differentiation of osteoblasts as well as secretion of type I collagen (20).

Disruption of PERK kinase activity in human tumor cell lines has been shown to increase apoptosis under hypoxia *in vitro* and impair tumor growth *in vivo* (21). Tumor cells experience episodes of hypoxia and nutrient deprivation during their growth due to inadequate blood supply and aberrant blood vessel function (22, 23). Thus, they are likely to be dependent on active UPR signaling to facilitate their growth. Consistent with this, mouse fibroblasts derived from $PERK^{-/-}$, $XBP1^{-/-}$, and $ATF4^{-/-}$ mice and fibroblasts expressing mutant eIF2α show reduced clonogenic growth and increased apoptosis under hypoxic conditions *in vitro* and reduced growth in mice (21, 23–25). In these studies, the regions of UPR activation coincided with hypoxic areas and exhibited higher rates of apoptosis. Further evidence supporting the role of PERK in promoting tumor growth was shown in transgenic mice expressing the SV40 T-antigen in the insulin-secreting beta cells, where insulinoma growth and vascularity was profoundly reduced in $PERK^{-/-}$ mice compared with wild-type controls (17). PERK and other UPR effectors regulate VEGF-A mRNA stability along with upregulation of VEGF-A and other proangiogenic factors under hypoxia or chemical stress (26).

Activation of the UPR has also been observed in human cervical carcinomas, glioblastomas (21), lung cancers (27), and breast cancers (28, 29). Thus, targeting various UPR-signaling components offers a novel therapeutic approach for cancers, especially those of secretory nature (adenocarcinoma, neuroendocrine tumors, and multiple myeloma) as well as those with greater hypoxia (pancreatic adenocarcinoma and glioblastoma). This manuscript describes the biologic characterization of a novel, highly selective inhibitor of PERK and its potential utility as an anticancer agent.

Materials and Methods

Reagents

GSK2656157 was synthesized at GlaxoSmithKline (GSK). It was dissolved in dimethyl sulfoxide (DMSO) to a stock concentration of 10 mmol/L, and stored in the dark at −20°C. Compound stock solution was thawed at room temperature before dilution into aqueous media at selected concentrations for use in biologic assays. For *in vivo* studies, GSK2656157 was formulated in 0.5% hydroxypropyl methyl cellulose, 0.1% tween-80 in water (pH 6.75). Tunicamycin (Molecular BioProducts), thapsigargin (Sigma-Aldrich), and cyclohexamide (Tocris Bioscience) were commercially obtained. EasyTag EXPRESS S^{35} Protein Labeling Mix, [^{35}S]-, 2 mCi (74 MBq) was purchased from Perkin Elmer.

NuPAGE SDS-PAGE, transfer solutions and consumables were purchased from Invitrogen. Odyssey blocking buffer was purchased from LI-COR Biosciences. RNeasy RNA isolation kits were purchased from Qiagen. Quantitative Pathway PCR Arrays were purchased from SABiosciences.

Animals

Eight- to twelve-week-old naive female CD-1, female nu/nu CD-1 mice (Charles River Laboratories) and severe combined immunodeficient (SCID) mice (Taconic Farms) were used. All animal studies were conducted after review by the Institutional Animal Care and Use Committee at GSK and in accordance with the GSK Policy on the Care, Welfare and Treatment of Laboratory Animals.

Cell lines and culture

Cell lines were purchased from the American Type Culture Collection and were routinely cultured in the recommended growth medium containing 10% FBS. All cell lines were maintained in humidified incubators at 37°C under 5% CO_2. The cell lines used in this study were not authenticated by any tests in our laboratory.

Kinase assay

Inhibitory potency of GSK2656157 was measured using recombinant GST-*PERK* (536–1116 amino acids) with 6-His-full-length human eIF2α as a substrate (30). Kinase selectivity was evaluated using 27 kinases at GSK as well as a panel of 300 kinases at Reaction Biology Corp.

Evaluation of PERK signaling induced by endoplasmic reticulum stress in human cells

BxPC3 (human pancreatic adenocarcinoma) or LL/2 (murine lung carcinoma) cells were treated with DMSO or various concentrations of GSK2656157 for 1 hour,

followed by addition of 5 μg/mL tunicamycin or 1 μmol/L thapsigargin for an additional 6 hours to induce endoplasmic reticulum-stress. Cells were lysed in cold radioimmunoprecipitation assay (RIPA) buffer [150 mmol/L NaCl, 50 mmol/L Tris-Cl pH 7.5, 0.25% sodium deoxycholate, 1% NP-40, protease inhibitors (Roche Diagnostics), and 100 mmol/L sodium orthovanadate (Sigma Aldrich)]. Clarified lysates were resolved by SDS-PAGE and transferred to nitrocellulose membrane using Invitrogen's NuPAGE system. Blots were incubated with antibodies to total PERK (R&D Systems), p-eIF-2α Ser51, total eIF-2α (Cell Signaling Technologies), ATF4, and CHOP (Santa Cruz Technologies). IRDye700DX-labeled goat anti-mouse immunoglobulin G (IgG), IRDye800-CW donkey anti-goat IgG, and IRDye800-CW goat anti-rabbit IgG (LI-COR Biosciences) were used as secondary antibodies. Proteins were detected on the Odyssey Infrared Imager (LI-COR Biosciences).

Measurement of *de novo* protein synthesis

BxPC3 cells were treated with DMSO or 1 μmol/L GSK2656157 for 1 hour before adding 5 μg/mL tunicamycin for an additional hour. Cells were metabolically labeled with 125 μCi ^{35}S-methionine for the subsequent 1 hour. Cells were lysed in cold RIPA buffer as previously described and lysates were resolved by SDS-PAGE, followed by exposure to a phosphorimager screen. Control cells were also pretreated with 100 μmol/L cyclohexamide for 1 hour followed by metabolic labeling. Radioisotope incorporation was quantitated using ImageQuant 5.2 software.

UPR gene expression profiling

BxPC3 cells were treated with DMSO or 1 μmol/L GSK2656157. One hour later, 5 μg/mL tunicamycin was added to the cells for an additional 6 hours followed by RNA isolation using the Qiagen RNeasy spin column method. Subsequent cDNA synthesis was conducted followed by quantitative PCR analysis using a human UPR PCR array developed by SABiosciences. Data analysis was conducted using manufacturer's online tools.

Pharmacodynamic studies

Naive female CD-1 mice were given a single oral dose of vehicle or GSK2656157. Animals were euthanized at various times, and blood and pancreas were collected. Frozen pancreas samples were homogenized in cold RIPA buffer. Lysates were resolved by SDS-PAGE and transferred to nitrocellulose membrane. Blots were incubated with antibodies against various antigens followed by secondary antibodies. Proteins were detected on the Odyssey Infrared Imager.

GSK2656157 concentrations were quantified in blood/water (1/1, v/v) and tissue homogenates by protein precipitation followed by high-performance liquid chromatography–tandem mass spectrometry analysis using positive-ion atmospheric pressure chemical ionization or Turbo Ionspray ionization (API4000 or API5000, Applied Biosystems). The lower limit of quantification of compound was as low as 1.0 nanogram per milliliter and the assays were linear over at least a 1,000-fold drug concentration range.

Effect on tumor vasculature

Vascular density of BxPC3 tumors treated with 50 or 150 mg/kg GSK2656157 (twice daily for 3 weeks) was analyzed using immunohistochemistry with rat anti-mouse pan-endothelial cell antigen (MECA-32, BD Biosciences) and anti-von Willerbrand factor (Dako). Effect on vascular perfusion was evaluated in mice bearing BxPC3 tumor xenografts using dynamic contrast enhanced (DCE)-MRI on days 0, 7, and 14 posttreatment with vehicle or GSK2656157 at 150 mg/kg, twice daily. Detailed methods are described in Supplementary Materials.

Histopathology of the mouse pancreas

Female CD-1 nude mice were treated with 150 mg/kg GSK2656157 (orally, twice daily) for 14 days and pancreas were harvested on days 15 and 29. Pancreas wet weights were taken for comparison. These tissues were then fixed in 10% neutral buffered formalin for 24 hours followed by paraffin embedding. Sections were cut (6 μmol/L) and stained with hematoxylin and eosin. Slides were reviewed by a pathologist and images taken at ×200 magnification.

In vivo efficacy studies

Exponentially growing HPAC (5×10^6 cells/mouse), Capan-2 (10×10^6 cells/mouse), or NCI-H929 (1×10^6 cells/mouse) cells were implanted subcutaneously into the right flank of 8- to 12-week-old female SCID mice. Similarly, 10×10^6 BxPC3 cells per mouse were implanted in female nude mice. When the tumors reached approximately 200 mm^3 in size, the animals were weighed, and block randomized according to tumor size into treatment groups of 8 mice each. Mice were dosed orally with the formulating vehicle or GSK2656157. Mice were weighed and tumors measured by calipers twice weekly. Tumor volumes were calculated using the formula: tumor volume = (Length × Width^2)/2. The percentage of tumor growth inhibition was calculated on each day of tumor measurement using the formula: 100× [1 − (average growth of the compound-treated tumors/average growth of vehicle-treated control tumors)].

Results

Kinase activity of GSK2656157

Recently, we reported the discovery of a series of potent and selective PERK inhibitors (30). Further medicinal chemistry optimization led to the identification of GSK2656157 (Table 1), a potent and selective inhibitor of PERK kinase with an IC_{50} of 0.9 nmol/L. In a panel of 300 kinase assays (Reaction Biology Corp), 44 were inhibited >50% at 10 μmol/L GSK2656157 (Supplementary Table S1). Fifteen of these kinases showed more than 80% inhibition at 10 μmol/L and were chosen together with EIF2AK3 (PERK), EIF2AK1 (HRI), EIF2AK2 (PKR), and GCN2 (S808G) for dose response (IC_{50}) analysis. In addition, IC_{50}'s were measured for available kinase assays in-house and for vascular endothelial growth factor receptor (VEGFRs). None of the kinases tested were inhibited at IC_{50}

Table 1. Structure and kinase selectivity of GSK2656157

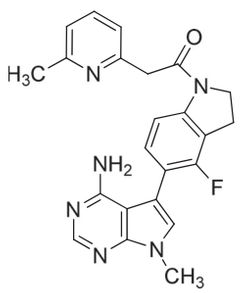

Kinase	IC_{50} (nmol/L)	Kinase	IC_{50} (nmol/L)
EIF2AK3 (PERK)	0.9	JAK2	24,547
EIF2AK1 (HRI)	460	ACK1	>10,000
BRK	822	MLK3	>10,000
EIF2AK2 (PKR)	905	TRKA	>10,000
MEKK2	954	MLK1	>10,000
Aurora B	1,259	FLT1	>10,000
KHS	1,764	KDR	>10,000
LCK	2,344	JNK1	>16,595
MLK2	2,796	RIPK2	>25,000
MEKK3	2,847	ASK1	>27,500
ALK5	3,020	BTK	>27,500
MLCK2	3,039	EGFR	>27,500
EIF2AK4 (GCN2)	3,162	GSK3B	>27,500
c-MER	3,431	IKK1	>27,500
PI3Kγ	3,802	IKK2	>27,500
WNK3	5,951	ITK	>27,500
LRRK2	6,918	JAK1, 3	>27,500
ROCK1	7,244	JNK3	>27,500
MSK1	8,985	p38α	>27,500
NEK1	9,807	PI3Kα, β, δ	>27,500
AXL	9,808	Aurora A	>27,500

values of 100 nmol/L or less confirming that GSK2656157 has outstanding selectivity for PERK inhibition (Table 1).

Cellular activity of GSK2656157

Cellular PERK-dependent signaling was measured in the BxPC3 pancreatic tumor cell line. PERK has been shown to be hyperactivated in cells upon treatment with pharmacologic agents that disturb the Ca^{2+} balance (thapsigargin), protein folding dithiothreitol (DTT), or glycosylation (tunicamycin) in the endoplasmic reticulum. Treatment of cells with tunicamycin (5 μg/mL) or thapsigargin (1 μmol/L) leads to activation and autophosphorylation of PERK, which was visualized by a mobility shift in Western blot analysis using anti-PERK antibodies, as there are no selective antibodies against human phospho-PERK. Pretreatment of cells with GSK2656157 resulted in inhibition of PERK activation as well as decreases in the downstream substrates, phospho-eIF2α, ATF4, and CHOP with an IC_{50} in the range of 10–30 nmol/L (Fig. 1A). Similar results were also obtained using DTT (5 mmol/L) in BxPC3 cells as well as all 3 UPR inducers in HPAC cells, another human pancreatic andenocarcinoma cell line (data not shown).

PERK activation results in the repression of global protein synthesis (31). Using a pulse-chase experimental approach, the effects of tunicamycin and GSK2656157 on *de novo* protein synthesis in BxPC3 cells were evaluated. Tunicamycin treatment caused a 36% reduction in ^{35}S-methionine incorporation compared with DMSO-treatment alone in the BxPC3 cells (Fig. 1B). Cells that were exposed to 1 μmol/L GSK2656157 before UPR induction were able to block this effect on *de novo* protein synthesis. These findings are consistent with PERK's role in maintaining cellular homeostasis under stress conditions.

Changes in RNA expression of 84 UPR-related genes was analyzed in BxPC3 cells. The excellent biochemical and cellular selectivity of GSK2656157 was also evidenced by lack of change in gene expression with GSK2656157 treatment compared with DMSO, in the absence of UPR induction (data not shown). Seventeen genes were found to be transcriptionally regulated (either up or down by ≥4-fold) in response to tunicamycin-induced UPR activation (Fig. 2). Five of these genes (*DDIT3, HERPUD1, PPP1R15A, C/EBP-beta*, and *ERN1*) were down-regulated more than 4-fold by GSK2656157, consistent with published reports using PERK siRNA (32).

Antiproliferative activity of GSK2656157 against multiple human tumor cell lines as well as primary human microvascular endothelial cells was evaluated in a 3-day proliferation assay using standard culture medium. In the absence of exogeneous UPR inducers, GSK2656157 had no significant effect on the growth of any of these cells with IC_{50} range of 6–25 μmol/L (data not shown), suggesting the UPR is inactive under normal cell culture conditions.

In vivo pharmacologic activity of GSK2656157 in mice

Demonstration of inhibition of PERK activation and downstream signaling with GSK2656157 in human xenograft models were unsuccessful due to the lack of available reagents (e.g., lack of phospho-specific antibodies to human PERK and Nrf2). However, a mouse-specific phospho-PERK antibody is available and was used to measure PERK inhibition in the mouse pancreas, where PERK is highly expressed and activated (31). As such, we chose to evaluate the naive mouse pancreas as a surrogate tissue to investigate the pharmacodynamic activity of GSK2656157 *in vivo* and correlate changes in phospho-PERK with pharmacokinetic properties.

The effect of GSK2656157 on Thr980 phosphorylation of endogenous pancreatic PERK in mice was assessed after a single oral administration of the compound. Complete inhibition of phospho-PERK Thr980 was observed through 8 hours after a single 50 mg/kg oral dose of GSK2656157 (Fig. 3A). Endogenous PERK activity was restored to almost normal levels by 18 hours. Interestingly, there was no effect on phospho-eIF2α (Ser51) level as a result of PERK inhibition. Concentrations of GSK2656157 in blood and pancreas tissue were similar and followed the same overall concentration-time profile (Fig. 3B). The lower blood and pancreas compound concentrations observed at 18 and 24 hours post-GSK2656157 administration correlates with the loss of effect

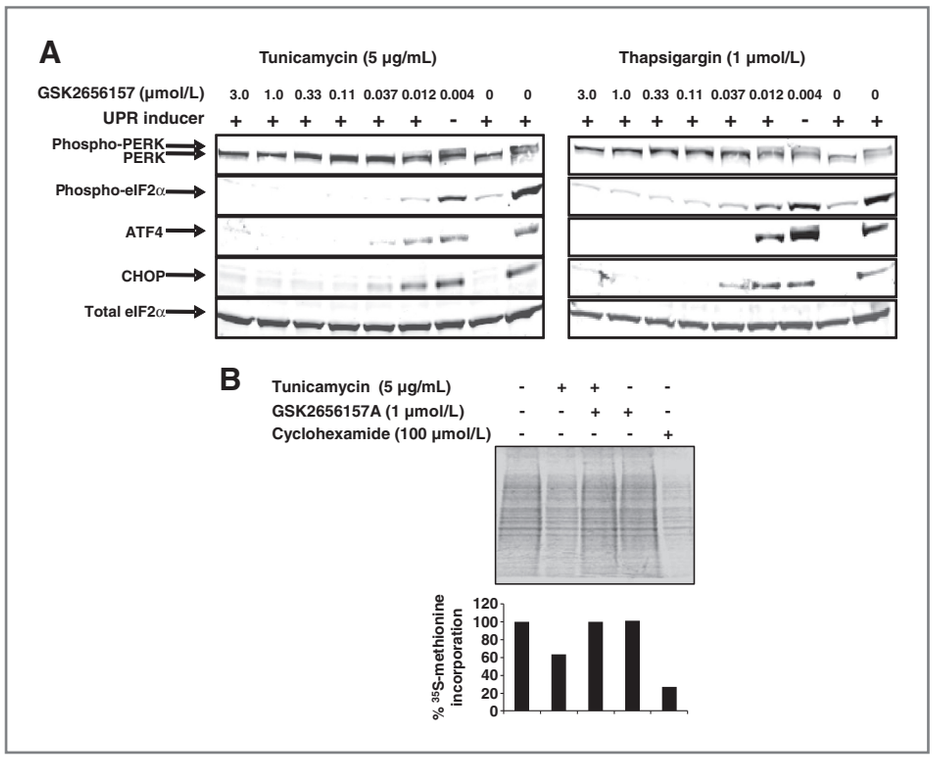

Figure 1. Cellular effect of GSK2656157 on PERK signaling and protein translation. A, BxPC3 cells were pretreated with different concentrations of GSK2656157 followed by UPR induction for 6 hours. Cell lysates were analyzed by Western blot analysis. B, BxPC3 cells were treated with GSK2656157, followed by tunicamycin and labeling with ^{35}S-methionine. Lysates were run on SDS-PAGE and analyzed using phosphorimager.

on basal phospho-PERK level. A dose response experiment using a single oral dose of GSK2656157 ranging from 1.5 to 150 mg/kg, followed 4 hours later with tissue collection resulted in dose-dependent inhibition of phospho-PERK Thr980 with more than 80% inhibition at 50 and 150 mg/kg (Supplementary Fig. S1).

Wolcott–Rallison syndrome patients and PERK$^{-/-}$ knockout mice exhibit permanent neonatal or early-infancy insulin-dependent diabetes (15, 31, 33). We thus evaluated the effect of GSK2656157 on the pancreas in naive female CD-1 mice. The wet weight of pancreas in mice was reduced by approximately 50% in mice following 150 mg/kg, twice daily for 14

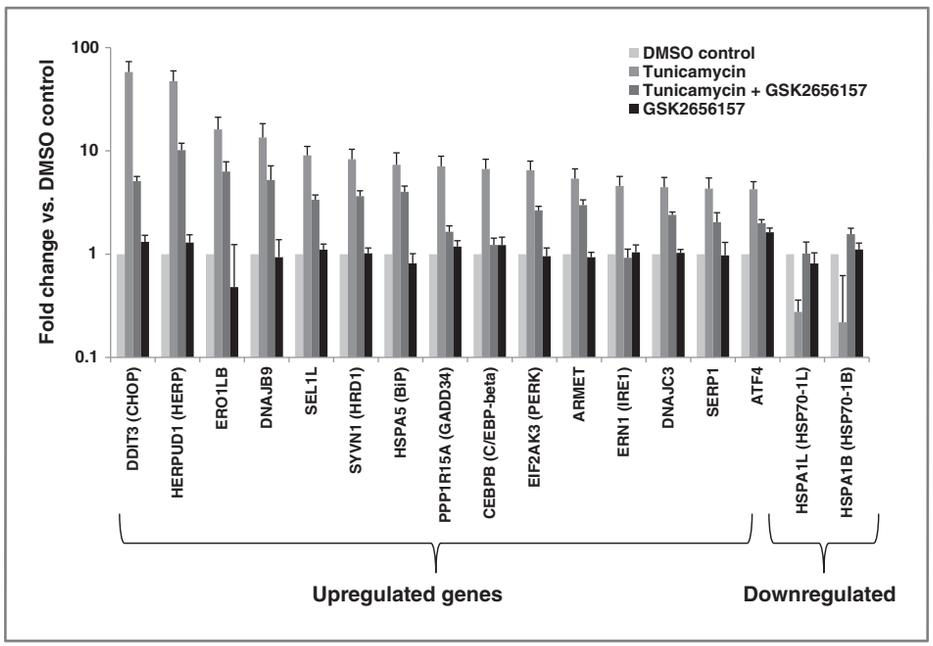

Figure 2. PERK inhibitor attenuates tunicamycin-induced UPR gene transcription. BxPC3 cells were treated with DMSO or 1 μmol/L GSK2656157 with and without tunicamycin and RNA expression of UPR-related genes was analyzed as described in Materials and Methods. Data represent mean fold change in RNA expression of genes significantly modulated by tunicamycin. Bars represent 95% confidence interval.

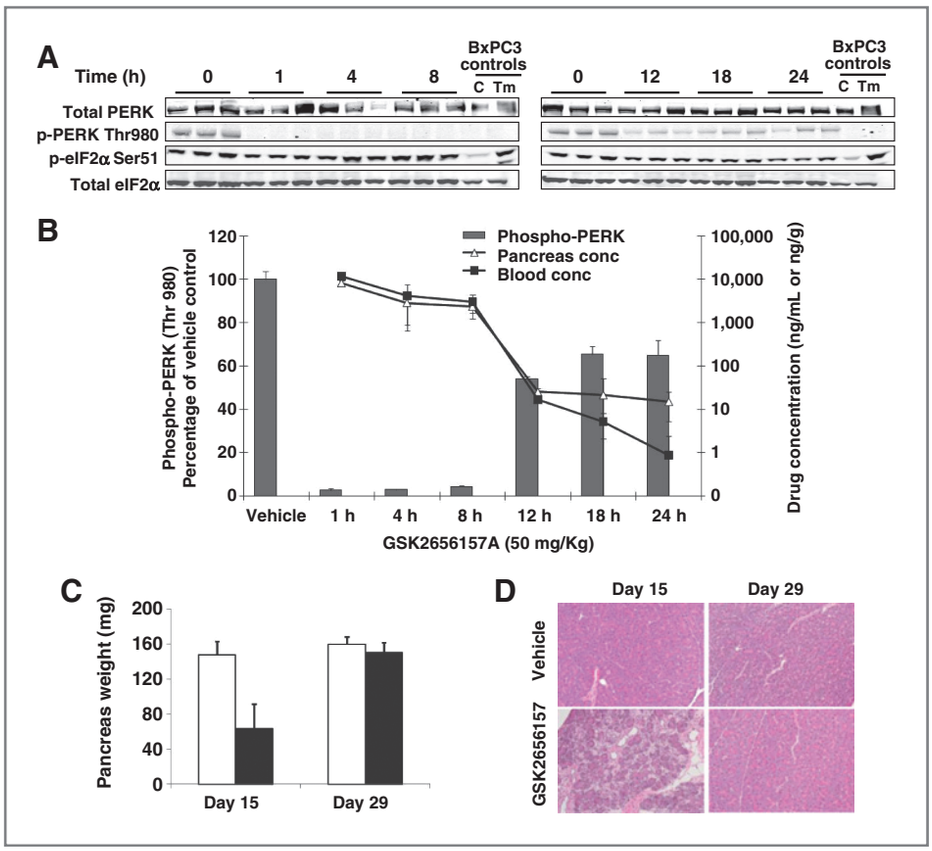

Figure 3. Pharmacodynamic effect of GSK2656157 on PERK in mouse pancreas. A and B, pharmacokinetic–pharmacodynamic analysis of PERK phosphorylation in the pancreas of mice treated with a single dose of GSK2656157. A, tissue lysates were analyzed for total and phospho-PERK and eIF2α by Western blot analysis. B, pharmacokinetic–pharmacodynamic correlation of phospho-PERK and drug concentration in blood and pancreas. Bars represent densitometric analysis of phospho-PERK, normalized to vehicle-treated control (mean ± SD). C and D, reversibility of histologic changes in pancreas of mice treated with PERK inhibitor. Mice were given 150 mg/kg GSK2656157 (twice daily) for 14 days. Pancreas were harvested and weighed on days 15 and 29. C, weight of pancreas tissues. Mean ± SD; $n = 4$ mice/group. Open bar, vehicle; dark bar, GSK2656157. D, representative hematoxylin and eosin sections of pancreas highlighting histologic changes with PERK inhibitor on day 15 and their reversibility on day 29 (14 days after 2 weeks of treatment).

days (Fig. 3C). Additional animals were included to observe recovery of the pancreas following drug discontinuation. Discontinuation of GSK2656157 for 2 weeks resulted in almost complete recovery of pancreas weight (Fig. 3C). Histopathologic analysis of pancreas sections showed degeneration and atrophy of exocrine acinar cells as well as degeneration of islet cells (Fig. 3D). These results are consistent with pancreatic changes observed in rats after 2 weeks of treatment with GSK2656157, where a decrease in proinsulin and insulin staining in beta cells was also observed (34). Similar to the recovery of the pancreas wet weight, histologic analysis confirmed almost complete recovery of acinar cell changes following a 2-week recovery period.

Antitumor activity of GSK2656157 *in vivo*

The ability of GSK2656157 to affect tumor growth *in vivo* was assessed in human tumor xenograft models of pancreatic cancer and multiple myeloma in immunocompromised mice. Treatment of mice with 50 or 150 mg/kg twice daily dosing of GSK2656157 resulted in dose-dependent inhibition of tumor growth in all four models; reaching 54–114% tumor growth inhibition at the 150 mg/kg, twice daily dose (Fig. 4). Differential sensitivity of these xenografts to the PERK inhibitor might be related to the intratumoral hypoxia and nutrient deprivation and/or other stresses. It is interesting to note that the most sensitive tumor xenograft (Capan2) grows slower than other 3 xenografts used, suggesting rate of tumor growth, a potential manifestation of various physiologic stresses, may be a reflection of dependency on PERK signaling.

As previously mentioned, we have been unsuccessful in demonstrating inhibition of the PERK phosphorylation in tumor xenograft studies due to a lack of antibodies against human phospho-PERK. We were also not able to detect any change in downstream signaling, such as phospho-eIF2α, ATF4, or CHOP levels in either mouse pancreas or tumor xenografts. Gene expression analysis in BxPC3 tumor xenografts showed statistically significant changes in RNA expression of very few genes, 11 of which were confirmed by real-time PCR analysis (*ASNS, PSAT1, CYP26A1, vWF, KNCF1, NES, KCNQ3, ZBED2, CDO1, TYR*). We evaluated the expression of these 11 genes in HPAC (pancreatic carcinoma) and RPMI-8226 (multiple myeloma) xenografts. Expression of Asparagine synthase (*ASNS*), phosphoserine aminotransferase 1 (*PSAT1*), and cytochrome P450 26A1 (*CYP26A1*) mRNA was increased in all 3 tumor models in samples treated with GSK2656157, whereas expression of von-Willebrand factor (vWF) was decreased in all 3 models (Supplementary Fig. S3). ASNS and PSAT1 regulate amino acid metabolism, whereas CYP26A1 is an endoplasmic reticulum membrane protein involved in retinoic acid metabolism. vWF is an endothelial cell marker and is likely reflective of changes in vascular density in GSK2656157-treated tumors. This is consistent with the emerging role of PERK in translational regulation of angiogenic genes (23). BxPC3 tumors from

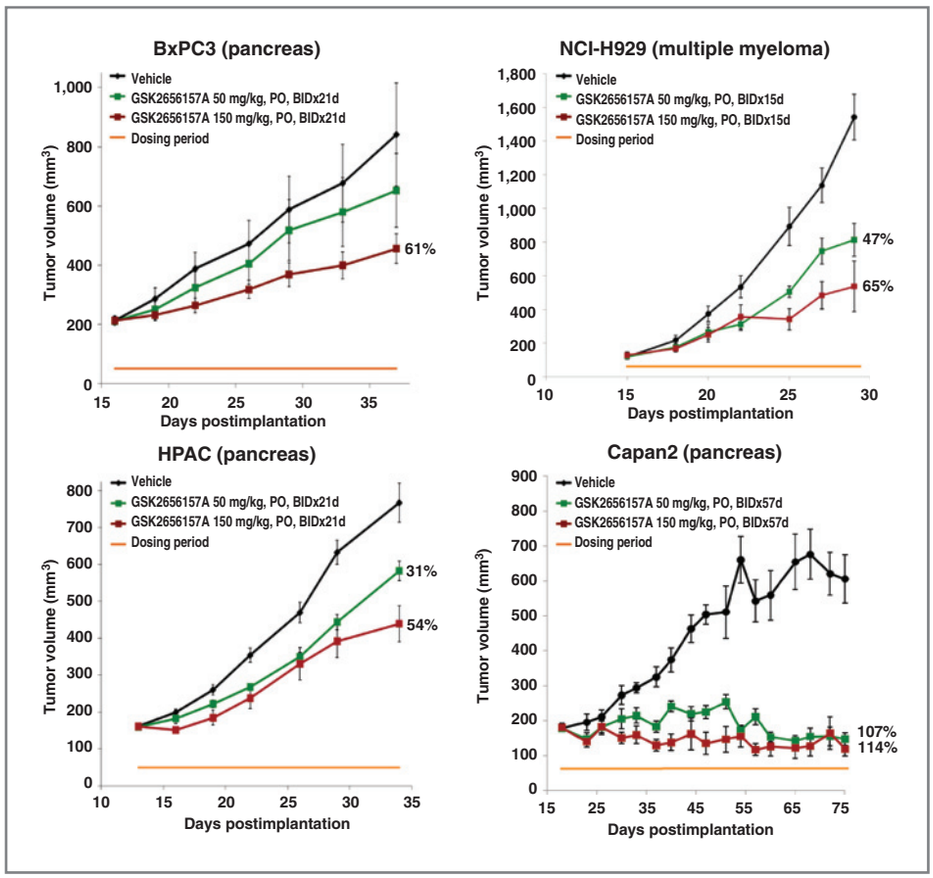

Figure 4. Antitumor activity of GSK2656157 *in vivo*. Mice bearing various human tumor xenografts were treated twice daily (BID) with vehicle (black) and GSK2656157 at 50 (green) or 150 mg/kg (red). Duration of treatment is shown by the horizontal orange line at the bottom of the graphs. Tumors were measured twice per week. Points, mean tumor volumes; bars, SE.

mice treated with GSK2656157 for 3 weeks were analyzed for vascular density by immunohistochemistry. There was a dose-dependent decrease in blood vessel density in tumors from mice treated with PERK inhibitor compared with vehicle-treated mice (Fig. 5A).

To further analyze the effect of PERK inhibition on vascular function, DCE-MRI imaging using Gd-diethylenetriaminepentaacetic acid (DTPA) was conducted in mice bearing BxPC3 tumor xenografts. Mice were treated with vehicle or 150 mg/kg GSK2656157, twice daily for 14 days. No mortality was observed in the vehicle group. Six mice treated with PERK inhibitor died between day 7 and day 14 posttreatment. Mortality was not observed in previous tumor growth experiments at this dose up to 57 days, suggesting that repeated anesthesia and other protocols associated with imaging might have contributed to the toxicity along with the compound treatment. One PERK inhibitor-treated mouse was excluded due to a failure of Gd-DTPA injection at baseline. K^{trans} values were significantly decreased in the GSK2656157-treated group from baseline to −72% at day 7, and −57% at day 14. In comparison, no significant differences were observed in the vehicle-treated group: +6.22% at day 7, and −4.47% at day 14 (Fig. 5B).

Discussion

Development of pharmacologic tools that selectively modulate an enzyme greatly facilitates the evaluation of the protein's biologic function and therapeutic potential. To our knowledge, GSK2656157 and related compounds are first in-class small molecule inhibitors of PERK, one of the key mediators of UPR signaling. Excellent biochemical potency against PERK, coupled with more that 100-fold selectivity over all 300+ kinases suggest that GSK2656157 can be used to evaluate the biologic function of PERK in various biologic contexts.

UPR signaling is believed to play a fundamental role in the establishment and maintenance of tumors, particularly those with severe hypoxia or with a secretory phenotype. Inhibition of PERK-dependent eIF2α phosphorylation has been implicated in translational control in response to cellular stresses such as an increase in misfolded proteins, nutrient deprivation, and hypoxia. GSK2656157 treatment potently inhibits phospho-eIF2α levels and subsequent *de novo* protein synthesis in response to chemically induced endoplasmic reticulum stress in multiple tumor cell lines. Phosphorylation of eIF2α also induces preferential translation of ATF4, a transcription activator of the integrated stress response. Consistent with earlier reports, the PERK/p-eIF2α/ATF4 pathway is required not only for translational control, but also for transcriptional activation of many genes, which critically regulate the UPR (Fig. 2). Induction of the UPR by various pharmacologic agents has been shown to activate all 3 arms of UPR in mammalian cells (PERK, IRE-1, and ATF6), however, the

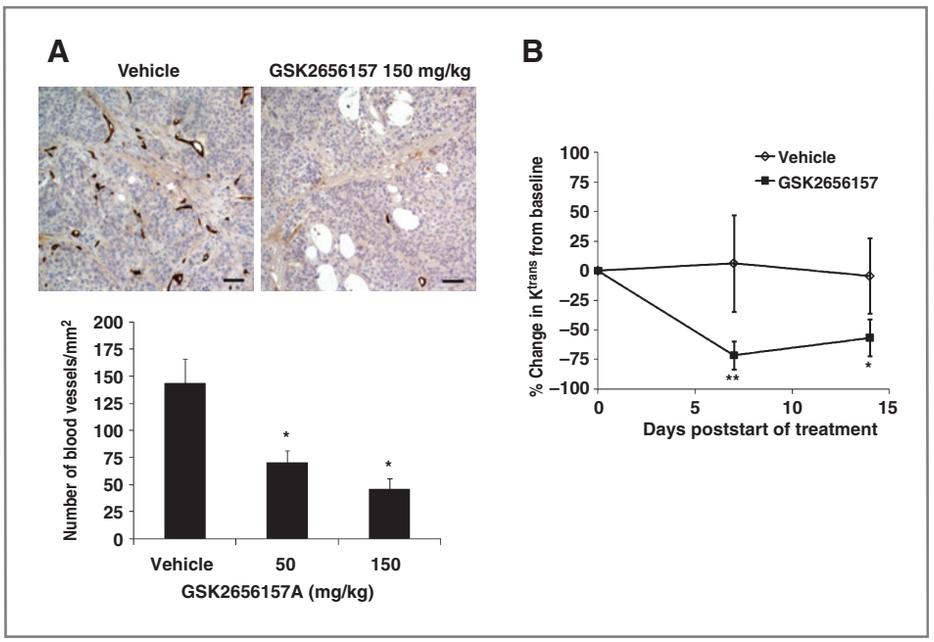

Figure 5. Vascular effects of GSK2656157 in tumor xenografts. A, effect on vascular density. BxPC3 tumor-bearing mice were treated twice daily for 21 days with GSK2656157. Tumor sections were analyzed for vascular density using immunohistochemistry for MECA and vWF (scale bar, 15 μm). Data in the graph represent mean ± SE ($n = 4$ mice/group); *, $P < 0.05$ (*t*-test). B, effect on vascular perfusion. Percentage changes in K^{trans} values from baseline DCE-MRI is shown as mean ± SE ($n = 5$ for GSK2656157; $n = 6$ for vehicle). Statistical analysis was conducted on the absolute median K^{trans} values using one-way ANOVA with *post hoc* Bonferroni test. **, $P < 0.01$; *, $P < 0.05$.

relative contribution of each or their interdependence is poorly understood. We therefore evaluated the effect of PERK inhibitor on the mRNA levels of 84 UPR-related genes in BxPC3 cells following tunicamycin treatment (see Supplementary Table S2 for full list of genes). Transcript levels of all 17 genes modulated by tunicamycin were attenuated to various degrees by GSK2656157, suggesting that transcriptional regulation of these genes is dependent on the activation of multiple pathways. The PERK inhibitor completely blocked tunicamycin-induced changes in expression of *PPP1R15A* (GADD34), *C/EBP-beta, ERN1 (IRE1), HSPA1L*, and *HSPA1B* genes, whereas the effect of PERK inhibition on the remaining genes was more modest. The latter data suggests that IRE1 or ATF6 activation under endoplasmic reticulum stress may regulate the expression of those genes, consistent with prior studies (35). Because tunicamycin-induced expression of IRE1 mRNA was completely blocked by PERK inhibition, it is possible that the inhibition of some of the mRNA changes by the PERK inhibitor is an indirect result of IRE1 regulation. Our data clearly shows that PERK regulates IRE1 by increasing its mRNA expression under endoplasmic reticulum stress, possibly via ATF4 transcription factor, thus highlighting the interdependence of various UPR signaling pathways for a concerted response.

To further characterize the *in vivo* pharmacologic activity of GSK2656157, we conducted multiple studies using the normal mouse pancreas. Endogenous PERK activation can be easily detected in this tissue using a commercially available rodent-specific phospho-PERK (Thr980) antibody. Treatment with GSK2656157 resulted in time- and dose-dependent inhibition of phospho-PERK. Because loss of PERK during embryonic development in mice results in severe dysfunction and cell death in both exocrine and endocrine pancreas, we evaluated the effect of GSK2656157 on pancreas tissue (12–14) Pharmacologic inhibition of PERK in adult mice caused damage to exocrine cells as well as pancreatic beta cells. These effects were also observed in rat and dog treated with GSK2656157 (data not shown), suggesting an evolutionarily conserved role of PERK in the homeostasis of pancreatic function.

Despite the potent inhibition of PERK activity in the mouse pancreas as shown by decrease in phospho-PERK and histologic changes, we were unable to show inhibition of canonical, downstream PERK signaling. No change in phospho-eIF2α, ATF, or CHOP protein levels was detected in pancreas of mice following GSK2656157 treatment. We do not see any change in PERK mobility on a Western blot analysis using antitotal PERK antibody in human tumor xenograft tissues from mice treated with GSK2656157 (data not shown), as observed in cell lines treated with tunicamycin or other endoplasmic reticulum stress inducers. Furthermore, using multiple technical approaches, we have also not been able to show PERK-dependent p-eIF2α, ATF4, or CHOP changes in these *in vivo* tumor models. It is very likely that other eIF2α kinases such as GCN2 contribute to the regulation of eIF2α in the context of the pancreas or tumor homeostasis. It is also speculated that PERK-dependent signaling may be limited to the very anoxic areas of the tumor and therefore difficult to detect by currently available technical methods. Gene expression results from tumor xenograft studies suggest that the PERK inhibitor GSK2656157 regulates amino acid metabolism and angiogenesis. ASNS and PSAT1 were previously reported to be regulated by PERK and the UPR (36, 37). Thus, even in the absence of measurable changes in canonical PERK signaling (PERK-eIF2α-ATF4-CHOP), protein homeostatsis might be impacted. Our results are consistent with endoplasmic reticulum stress independent role of PERK in tumor physiology, as shown for beta cell proliferation, pancreatic exocrine cell viability, and proliferation and differentiation of osteoblasts (13, 14, 20).

Similarly, PERK plays a role in trafficking and secretion of proinsulin and type I collagen in beta cells and osteoblasts, respectively (18–20). Further studies to understand molecular mechanism(s) of transcriptional regulation of ASNS and PSAT1 by PERK will be required to define any shared function in these various cell types.

Consistent with our primary hypothesis, treatment of mice with GSK2656157 resulted in inhibition of tumor growth in multiple human tumor xenografts. Our results are also consistent with earlier studies showing reduced growth of tumors lacking the PERK gene (17, 21). Altered amino acid metabolism and angiogenesis appear to be the primary effector mechanism of antitumor activity. Activation of both PERK and IRE1 has been shown to regulate angiogenesis (23, 38), and our data showing the reduction in vascular density as well as a decrease in vascular perfusion in tumor xenograft in mice treated with GSK2656157 further validates the role of PERK in tumor angiogenesis. Angiogenesis inhibitors have shown clinical success in the treatment of patients with multiple cancers, however, most of these patients relapse. A PERK inhibitor may offer a therapeutic advantage by acting on another (yet undefined) node of angiogenic signaling. Given the on-target pharmacologic effects of PERK inhibitor on exocrine and endocrine pancreas, development of any PERK inhibitor in human subjects would need to be cautiously pursued in patients with greatest unmet medical need and where pancreatic function may already be compromised, for example, a subset of pancreatic cancer patients.

Disclosure of Potential Conflicts of Interest

Elisabeth A Minthorn is employed in GlaxoSmithKline as a head/team leader and has ownership interest (including patents) in GlaxoSmithKline stock. Beat M Jucker has ownership interest (including patents) in GlaxoSmithkline. No potential conflicts of interest were disclosed by the other authors.

Authors' Contributions

Conception and design: C. Atkins, E.A. Minthorn, K.G. Moss, H. Alsaid, J.M. Axten, R. Kumar

Development of methodology: C. Atkins, S.Y. Zhang, K.G. Moss, T.B. Stanley, B.M. Jucker

Acquisition of data (provided animals, acquired and managed patients, provided facilities, etc.): C. Atkins, E.A. Minthorn, S.Y. Zhang, D.J. Figueroa, K.G. Moss, N. Gaul, A.E. Choudhry, H. Alsaid

Analysis and interpretation of data (e.g., statistical analysis, biostatistics, computational analysis): C. Atkins, E.A. Minthorn, D.J. Figueroa, K.G. Moss, B. Sanders, A. Goetz, N. Gaul, A.E. Choudhry, H. Alsaid, B.M. Jucker, R. Kumar

Writing, review, and/or revision of the manuscript: C. Atkins, E.A. Minthorn, D.J. Figueroa, K.G. Moss, A. Goetz, H. Alsaid, B.M. Jucker, J.M. Axten, R. Kumar

Administrative, technical, or material support (i.e., reporting or organizing data, constructing databases): C. Atkins, Q. Liu, S.Y. Zhang, D.J. Figueroa, K.G. Moss

Study supervision: C. Atkins, E.A. Minthorn, S.Y. Zhang, H. Alsaid, R. Kumar

The costs of publication of this article were defrayed in part by the payment of page charges. This article must therefore be hereby marked *advertisement* in accordance with 18 U.S.C. Section 1734 solely to indicate this fact.

Received August 7, 2012; revised December 10, 2012; accepted December 31, 2012; published OnlineFirst January 18, 2013.

References

1. Koumenis C, Wouters BG. "Translating" tumor hypoxia: unfolded protein response (UPR)-dependent and UPR-independent pathways. Mol Cancer Res 2006;4:423–36.
2. Ma Y, Hendershot LM. The role of the unfolded protein response in tumour development: friend or foe? Nat Rev Cancer 2004;4:966–77.
3. Feldman DE, Chauhan V, Koong AC. The unfolded protein response: a novel component of the hypoxic stress response in tumors. Mol Cancer Res 2005;3:597–605.
4. Hamanaka RB, Bobrovnikova-Marjon E, Ji X, Liebhaber SA, Diehl JA. PERK-dependent regulation of IAP translation during ER stress. Oncogene 2009;28:910–20.
5. Ma Y, Hendershot LM. The mammalian endoplasmic reticulum as a sensor for cellular stress. Cell Stress Chaperones 2002;7:222–9.
6. Shi Y, Vattem KM, Sood R, An J, Liang J, Stramm L, et al. Identification and characterization of pancreatic eukaryotic initiation factor 2a-subunit kinase, PEK, involved in translational control. Mol Cell Biol 1998;18:7499–509.
7. Sood R, Porter AC, Olsen DA, Cavener DR, Wek RC. A mammalian homologue of GCN2 protein kinase important for translational control by phosphorylation of eukaryotic initiation factor-2a. Genetics 2000;154:787–801.
8. Ma Y, Lu Y, Zeng H, Ron D, Mo W, Neubert TA. Characterization of phosphopeptides from protein digests using matrix-assisted laser desorption/ionization time-of-flight mass spectrometry and nanoelectrospray quadrupole time-of-flight mass spectrometry. Rapid Commun Mass Spectrom 2001;15:1693–700.
9. Su Q, Wang S, Gao HQ, Kazemi S, Harding HP, Ron D, et al. Modulation of the eukaryotic initiation factor 2 alpha-subunit kinase PERK by tyrosine phosphorylation. J Biol Chem 2008;283:469–75.
10. Marciniak SJ, Garcia-Bonilla L, Junjie Hu J, Harding HP, Ron D. Activation-dependent substrate recruitment by the eukaryotic translation initiation factor 2 kinase PERK. J Cell Biol 2006;172:201–9.
11. Cullinan SB, Diehl JA. PERK-dependent activation of Nrf2 contributes to redox homeostasis and cell survival following ER stress. J Biol Chem 2004;279:20076–87.
12. Harding HP, Zeng H, Zhang Y, Jungreis R, Chung P, Plesken H, et al. Diabetes mellitus and exocrine pancreatic dysfunction in PERK$^{-/-}$ mice reveals a role for translational control in survival of secretory cells. Mol Cell 2001;7:1153–63.
13. Zhang W, Feng D, Li Y, Iida K, McGrath B, Cavener DR. PERK EIF2AK3 control of pancreatic β cell differentiation and proliferation is required for postnatal glucose homeostasis. Cell Metabol 2006;4:491–7.
14. Iida K, Li Y, McGrath BC, Frank A, Cavener DR. PERK eIF2 alpha kinase is required to regulate the viability of the exocrine pancreas in mice. BMC Cell Biol 2007;8:1–16.
15. Senee V, Vattem KM, Delepine M, Rainbow LA, Haton C, Lecoq A, et al. Wolcott-Rallison syndrome: clinical, genetic, and functional study of EIF2AK3 mutations and suggestion of genetic heterogeneity. Diabetes 2004;53:1876–83.
16. Julier C, Nicolino M. Wolcott–Rallison syndrome. Orphanet J Rare Dis 2010;5:1–13.
17. Gupta S, McGrath B, Cavener DR. PERK regulates the proliferation and development of insulin-secreting beta-cell tumors in the endocrine pancreas of mice. PLoS ONE 2009;4:1–6.
18. Cavener DR, Gupta S, McGrath BC. PERK in beta cell biology and insulin biogenesis. Trends Endocrinol Metabol 2010;21:714–21.
19. Gupta S, McGrath B, Cavener DR. PERK (EIF2AK3) regulates proinsulin tranfficking and quality control in the secretory pathway. Diabetes 2010;59:1937–47.
20. Wei J, Sheng X, Feng D, McGrath B, Cavener DR. PERK is essential for neonatal skeletal development to regulate osteoblast proliferation and differentiation. J Cell Physiol 2008;217:693–707.
21. Bi M, Naczki C, Koritzinsky M, Fels D, Blais J, Hu N, et al. ER stress-regulated translation increases tolerance to extreme hypoxia and promotes tumor growth. EMBO J 2005;24:3470–81.

22. Brown J, Giaccia A. The unique physiology of solid tumors: opportunities (and problems) for cancer therapy. Cancer Res 1998;58:1408–16.
23. Blais JD, Addison CL, Edge R, Falls T, Zhao H, Wary K, et al. Perk-dependent translational regulation promotes tumor cell adaptation and angiogenesis in response to hypoxic stress. Mol Cell Biol 2006;26: 9517–32.
24. Koumenis C, Naczki C, Koritzinsky M, Rastani S, Diehl A, Sonenberg N, et al. Regulation of protein synthesis by hypoxia via activation of the endoplasmic reticulum kinase PERK and phosphorylation of the translation initiation factor eIF2α. Mol Cell Biol 2002;22:7405–16.
25. Romero-Ramirez LH, Cao H, Nelson D, Hammond E, Lee AH, Yoshida H, et al. XBP1 is essential for survival under hypoxic conditions and is required for tumor growth. Cancer Res 2004;64:5943–7.
26. Ghosh R, Lipson KL, Sargent KE, Mercurio AM, Hunt JS, Ron D, et al. Transcriptional regulation of VEGF-A by the unfolded protein response pathway. PLoS ONE 2010;5:1–12.
27. Jorgensen E, Stinson A, Shan L, Yang J, Gietl D, Albino AP. Cigarette smoke induces endoplasmic reticulum stress and the unfolded protein response in normal and malignant human lung cells. BMC Cancer 2008;8:1–30.
28. Ameri K, Lewis CE, Raida M, Sowter H, Hai T, Harris AL. Anoxic induction of ATF-4 through HIF-1-independent pathways of protein stabilization in human cancer cells. Blood 2004;103:1876–82.
29. Davies MPA, Barraclough DL, Stewart C, Joyce KA, Eccles RM, Barraclough R, et al. Expression and splicing of the unfolded protein response gene XBP-1 are significantly associated with clinical outcome of endocrine-treated breast cancer. Int J Cancer 2008;123:85–8.
30. Axten JM, Medina JR, Feng Y, Shu A, Romeril SP, Seth WG, et al. Discovery of 7-methyl-5-(1-{[3- (trifluoromethyl)phenyl]acetyl}-2, 3-dihydro-1H-indol-5-yl)-7H-pyrrolo[2,3-d]pyrimidin-4-amine (GSK2606414), a potent and selective first-in-class inhibitor of PKR-like endoplasmic reticulum kinase (PERK). J Med Chem 2012; 55:7193–207.
31. Zhang P, McGrath B, Li S, Frank A, Zambito F, Reinert J, et al. The PERK eukaryotic initiation factor 2α kinase is required for the development of the skeletal system, postnatal growth, and the function and viability of the pancreas. Mol Cell Biol 2002;22:3864–74.
32. Teske BF, Baird TD, Wek RC. Methods for analyzing eIF2 kinases and translational control in the unfolded protein response. Methods Enzymol 2011;490:333–56.
33. Harding HP, Zhang Y, Ron D. Protein translation and folding are coupled by an endoplasmic-reticulum-resident kinase. Nature 1999;397:271–4.
34. Gales T, Ringenberg M, Mirabile R, Kane J, Hart T, Laffan S, et al. PERK inhibitor induces pancreatic toxicity in rats. Soc Tox Path 2012, Abs#87.
35. Lee A-H, Iwakoshi NN, Glimcher LH. XBP-1 regulates a subset of endoplasmic reticulum resident chaperone genes in the unfolded protein response. Mol Cell Biol 2003;23:7448–59.
36. Gjymishka A, Su N, Kilberg MS. Transcriptional induction of the human asparagine synthetase gene during the unfolded protein response does not require the ATF6 and IRE1/XBP1 arms of the pathway. Biochem J 2009;417:695–703.
37. Bull VH, Thlede B. Proteome analysis of tunicamycin-induced ER stress. Electrophoresis 2012;33:1814–23.
38. Drogat B, Auguste P, Nguyen DT, Bouchecareilh M, Pineau R, Nalbantoglu I, et al. IRE1 signaling is essential for ischemia-induced vascular endothelial growth factor-a expression and contributes to angiogenesis and tumor growth *in vivo*. Cancer Res 2007;67:6700–7.